The C2 Catalytic Domain of Adenylyl Cyclase Contains the Second Metal Ion (Mn^{2+}) Binding Site†

Thomas Mitterauer,‡ Martin Hohenegger,‡ Wei-Jen Tang,§ Christian Nanoff,‡ and Michael Freissmuth*,‡

Institute of Pharmacology, University of Vienna, A-1090 Vienna, Austria, and Department of Pharmacological and Physiological Sciences, University of Chicago, Chicago, Illinois 60637

Received June 17, 1998; Revised Manuscript Received September 22, 1998

ABSTRACT: Membrane-bound mammalian adenylyl cyclase isoforms contain two internally homologous cytoplasmic domains (C1 and C2). When expressed separately, C1 and C2 are catalytically inactive, but conversion of ATP to cAMP is observed if C1 and C2 are combined. By analogy with DNA polymerases, adenylyl cyclases are thought to require two divalent metal ions for nucleotide binding and phosphodiester formation; however, only one Mg^{2+} ion (liganded to C1) has been visualized in the recently solved crystal structure of a C1−C2 complex [Tesmer, J. J. G., Sunahara, R. K., Gilman, A. G., and Sprang, S. R. (1997) *Science 278*, 1907−1916]. Here, we have studied the binding of ATP to IIC2 (from type II adenylyl cyclase) using ATP analogues [2′,3′-dialdehyde ATP (oATP), a quasi-irreversible inhibitor that is covalently incorporated via reduction of a Schiff base, the photoaffinity ligand 8-azido-ATP ($^8N_3$-ATP), and trinitrophenyl-ATP (TNP-ATP), a fluorescent analogue] and fluorescein isothiocyanate (FITC). [α-^{32}P]-oATP and ^{8}N-[α-^{32}P]ATP are specifically incorporated into IIC2. Labeling of IIC2 by [α-^{32}P]oATP and by FITC is greatly enhanced by Mn^{2+} and to a much lesser extent by Mg^{2+}. Similarly, TNP-ATP binds to IIC2 as determined by fluorescence enhancement, and this binding is promoted by Mn^{2+}. Thus, a second metal ion binding site (preferring Mn^{2+}) is contained within the C2 domain, and this finding highlights the analogy in the reaction catalyzed by DNA polymerases and adenylyl cyclases.

In mammalian cells, the ubiquitous second-messenger cAMP is generated from ATP by a family of membrane-bound adenylyl cyclases. At least nine different mammalian isoforms have been identified (for a review, see ref *1*). They are activated by $G_{s\alpha}$, the α-subunit of the stimulatory heterotrimeric G protein G_S, and the hypotensive diterpene forskolin, although individual isoforms differ in their sensitivity to these activators. Additional regulators, which affect some, but not all, isozymes, include α-subunits of the $G_i/G_o/G_z$ subgroup of G proteins, G protein $\beta\gamma$-dimers, Ca^{2+}, Ca^{2+}-liganded calmodulin, and protein kinase-dependent phosphorylases. Finally, catalysis can also be inhibited by adenosine and adenosine analogues, in which the ribose may be altered (by dehydroxylation or phosphorylation); because substitutions are not tolerated on the purine ring, these inhibitors are referred to as P-site inhibitors (*2*). The deduced sequence of all isoforms predicts a complex topology; two hydrophobic cores comprised of six putative transmembrane-spanning helices each are connected by an intracellular domain of about 40 kDa. A second large intracellular portion is at the carboxy terminus; these two domains are internally homologous over a stretch of ∼200 amino acids. The hydrophobic portions are dispensable for enzymatic activity. The intracellular, highly conserved domains (referred to as C1 and C2)[1] suffice to catalyze the formation of cAMP. Either domain is catalytically inactive, but forskolin- and $G_{s\alpha}$-stimulated conversion of ATP to cAMP is observed if C1 and C2 are either expressed as a fusion protein (*3*, *4*) or synthesized separately and combined (*5*−*7*). Thus, although C1 and C2 each form homodimers (*7*, *8*), only a heterodimer composed of a C1 and a C2 domain is capable of efficient catalysis. Activation of the enzyme by the physiological regulator $G_{s\alpha}$ and forskolin can, at least in part, be attributed to their ability to promote association of C1 and C2 (*7*). In addition, a reorientation of the active site is likely to occur (*9*, *10*).

Adenylyl cyclase uses Mg·ATP or Mn·ATP as the substrate, but a divalent metal ion (Mg^{2+} or Mn^{2+}) is required in excess of ATP (*11*). This suggests that two metal ions are present in the active site. However, in the recently elucidated structure of a C1−C2 heterodimer complexed to a P-site inhibitor and pyrophosphate, only a single Mg^{2+} is seen, and this is bound to a pair of aspartate residues in C1 (*9*). Nevertheless, the C1 heterodimer is inactive, while C2 alone displays, an exceedingly low but detectable, catalytic

†This work was supported by grants from the Austrian Science Foundation (FWF-P12750) and from the EU-sponsored ENBST to M.F. and from the Science Foundation of the Austrian National Bank to M.H. (6646).

* To whom correspondence should be addressed: Institute of Pharmacology, Vienna University, Währinger Strasse 13a, A-1090 Vienna, Austria. Phone: 43-1-40 480/298. Fax: 43-1-402 48 33. E-mail: michael.freissmuth@univie.ac.at.

‡ University of Vienna.

§ University of Chicago.

[1] Abbreviations: IC1 and IIC2, first and second intracellular domains of type I and type II mamamlian adenylyl cyclase, respectively, that comprise the catalytic site; oATP, 2′,3′-dialdehyde-ATP; Bz_2ATP, 3′-*O*-(4-benzoyl)benzoyl-ATP; $^8N_3$-ATP, 8-azido-ATP; 2′,3′-ddA, 2′,3′-dideoxyadenosine; DDT, dithiothreitol; FITC, fluorescein isothiocyanate; $rG_{s\alpha-s}$, recombinant short splice variant of the GTP-binding protein that stimulates adenylyl cyclase; TNP-ATP, 2′,3′-*O*-(2,4,6-trinitrophenyl)-ATP.

10.1021/bi981441m CCC: $15.00
Published on Web 10/28/1998

activity (*3*). In this work, we have therefore focused on the binding of ATP analogues to C2. Our experiments show that isolated C2 can per se bind ATP analogues albeit with low affinity; binding of ATP analogues to C2 is enhanced by Mn^{2+}.

MATERIALS AND METHODS

Materials. [α-^{32}P]ATP and [^{3}H]cAMP were from Dupont NEN (Boston, MA). $^{8}N_3$-[α-^{32}P]ATP and unlabeled $^{8}N_3$-ATP were from ICN (Irvine, CA). ATP and GTPγS were purchased from Boehringer-Mannheim (Mannheim, FRG). Forskolin, adenosine, and 2′,3′-ddA were from Sigma-Aldrich (St. Louis, MO). Sephadex LH20 and Sephadex G10 as well as Mono-Q were from Pharmacia (Uppsala, Sweden). Ni−NTA agarose was from Qiagen (Hilden, FRG). FITC and TNP-ATP were from Molecular Probes (Leiden, The Netherlands). Reagents for electrophoresis were from Bio-Rad (Richmond, CA). 2′,3′-Dialdehyde-ATP (oATP) was prepared by periodate oxidation according to the work of Easterbrook-Smith et al. (*12*) and purified as previously described (*13*). [α-^{32}P]oATP was prepared in a similar way using 250 μCi of [α-^{32}P]ATP, to which 200 nmol of unlabeled ATP was added as a carrier. Bz_2ATP and Bz_2-[α-^{32}P]ATP were synthesized and purified as described by Williams and Coleman (*14*). The yield of purified Bz_2ATP was ∼15%.

Preparation of Platelet Membranes and Purification of IIC2. Membranes were prepared from human platelets as described previously (*15*). *Escherichia coli* BL21DE3 cells were transformed with a plasmid encoding IIC2 tagged with hexahistidine to allow for its purification by metal-chelating chromatography (*6*). The protein concentration was determined by dye binding with Coomassie Blue using bovine serum albumin as the standard; the molar amount of IIC2 was estimated from the protein concentration using a molecular mass of 30 kDa.

Determination of Adenylyl Cyclase Activity. Adenylyl cyclase activity in platelet membranes (5−30 μg of protein/assay) was measured as described previously (*15*) in the presence of ATP (10 μM to 2 mM), 50 μM forskolin, and 10 mM $MgCl_2$ for 10−30 min at 25 °C. In some experiments, adenylyl cyclase activity in platelet membranes was irreversibly inactivated by preincubation with oATP; platelet membranes (∼0.15 mg) were resuspended in buffer containing 50 mM Hepes·NaOH (pH 7.5), 1 mM EDTA, 10 mM $MgCl_2$, 1 mM ATP, or 1 mM oATP, in the absence and presence of forskolin (50 μM) for 20 min at 20 °C. Where indicated, $NaCNBH_3$ (100 mM final concentration, 1 min on ice) and $NaBH_4$ (10 mM, additional 10 min on ice) were added sequentially to the suspension (*16*). Thereafter, the suspension was diluted 10-fold in buffer lacking ATP analogues and forskolin, and the membranes were recovered by centrifugation (10 min at 50000*g*). After two washes, the membranes were resuspended in 30 μL of buffer, the protein level was measured, and adenylyl cyclase activity was determined. Adenylyl cyclase activity of IIC2 (0.05−0.5 μg of each/assay) was measured in the presence of IC1 (0.1 μg/assay) in 50 μL of buffer [50 mM Hepes·NaOH (pH 7.5), 1 mM EDTA, 1 mM DTT, and 10 mM $MgCl_2$] in the presence of 0.05−5 mM ATP and 0.1 mM forskolin. If not otherwise indicated, the incubation was carried out for 10 min at 20 °C.

Covalent Labeling of IIC2 with ATP Analogues and FITC. IIC2 (∼0.5−2 μg/reaction) was incubated for 20 min at 20 °C in 20 μL of buffer [50 mM Hepes·NaOH (pH 7.5), 1 mM EDTA, and 10 mM $MgCl_2$] containing 80 μM Bz_2[α-^{32}P]ATP (specific activity of ∼100−500 cpm/pmol), 100 μM [α-^{32}P]oATP (specific activity of ∼100−500 cpm/pmol), or 40 μM $^{8}N_3$-[α-^{32}P]ATP (specific activity of ∼2000−4000 cpm/pmol). For [α-^{32}P]oATP, the incorporation was catalyzed by the sequential addition of $NaCNBH_3$ and $NaBH_4$ which gave final concentrations of 100 (1 min on ice) and 10 mM (additional 10 min on ice), respectively (*17*). The reaction mixtures with Bz_2[α-^{32}P]ATP and $^{8}N_3$-[α-^{32}P]ATP were irradiated ($\lambda = 254$ nm, 100 W UV lamp placed 5 cm above the reaction tubes) for 1 min on ice. Laemmli sample buffer (4-fold concentrated and containing 80 mM DTT) was added; the samples were boiled and applied to SDS−polyacrylamide gels. To determine the stoichiometry of [α-^{32}P]oATP incorporation, IIC2 (20 μg) was incubated in 25 μL of buffer [50 mM Hepes·NaOH (pH 7.5), 1 mM EDTA, and 5 mM $MnCl_2$] with [α-^{32}P]oATP concentrations ranging from 0.1 to 3 mM (specific activity of 20−170 cpm/pmol). After 20 min at 20 °C, $NaCNBH_3$ and $NaBH_4$ were added as described above; the protein was denaturated by the addition of 0.5 mL of 2% SDS and 0.5 mL of 30% trichloroacetic acid. The precipitate was poured onto nitrocellulose filter (NC45, Schleicher & Schuell), which had been presoaked in 1 mM unlabeled oATP. The filters were washed with 18 mL of 6% trichloroacetic acid. The radioactivity retained on the filters was determined by liquid scintillation counting. The filter blank was determined in the absence of IIC2 and amounted to about 1% of the total radioactivity added.

FITC was dissolved in DMF to yield a 50 mM stock solution and stored at −20 °C. For protein labeling, FITC was diluted to 10 mM in DMSO and used immediately. The final concentration of FITC in the labeling reaction was 0.1 mM; preliminary experiments verified that the carryover of solvents did not affect adenylyl cyclase activity. IC1 or IIC2 (each at ∼0.5−2 μg/reaction) was incubated with 0.1 mM FITC in 20 μL of buffer [20 mM Hepes·NaOH (pH 8.0) and 1 mM EDTA] in the absence and presence of the indicated concentrations of $MgCl_2$, $MnCl_2$, and ATP analogues for 15 min at 20 °C in the dark. The reaction was stopped by the addition of Laemmli sample buffer (4-fold concentrated and containing 80 mM DTT). The proteins were resolved by electrophoresis on an SDS−polyacrylamide gel. Thereafter, the unreacted FITC (which migrates with the dye front) and the labeled protein bands were visualized by placing the gel on an UV transilluminator; the picture was recorded, and the fluorescence was quantitated with a Gel Doc 1000 Video Documentation System (Bio-Rad). Subsequently, the gel was stained with Coomassie Blue to confirm that equal amounts of the protein had been loaded onto each individual lane.

Fluorescence Measurements. Fluorescence spectra were recorded on a Hitachi F-4500 fluorescence spectrophotometer. All measurements were taken while the solution was continuously stirred at room temperature in a 5 mm × 5 mm cuvette (0.15 mL minimum volume); reagents were applied in small volumes (2−10 μL) through the closed lid by injection with Hamilton syringes. Three-dimensional spectra were recorded with all components (including TNP-

ATP in dimethylformamide) so the excitation and emission wavelength peaks could be identified. The slit widths on the excitation and emission monochromators were 5 nm; the instrument response was set at 10 ms and the photomultiplier voltage at 700 and 950 V for recordings taken at 20−60 and 5−20 μM IIC2, respectively. The excitation wavelength was 408 nm, in the time scan mode; the emission wavelength was 540 nm. All recordings were taken in 0.2−0.25 mL of buffer containing 20 mM Hepes (pH 7.5) and 1 mM EDTA; the concentrations of IIC2, TNP-ATP, ATP, adenosine, $MnCl_2$, and $MgCl_2$ are indicated in the figure legends. Neither ATP nor adenosine (or 2′,3′-ddA) quenched the fluorescence of TNP-ATP in 20% dimethylformamide.

RESULTS

Inhibition of Adenylyl Cyclase Activity by 2′,3′-Dialdehyde-ATP. The ATP analogue 2′,3′-dialdehyde-ATP (oATP) lacks a free 3′-hydroxyl group on the modified ribose ring; hence, oATP cannot serve as a substrate for adenylyl cyclase but ought to inhibit catalysis, if it binds to adenylyl cyclase. This was verified by determining adenylyl cyclase activity in platelet membranes or with the combination of the domains IC1 and IIC2. In platelet membranes, oATP inhibited cAMP formation in a monophasic manner with an IC_{50} value of 193 ± 15 μM in the presence of 50 μM ATP (■ in Figure 1A); if the concentration of ATP was raised to 500 μM (● in Figure 1A), the inhibition curve for oATP shifted to the right (IC_{50} = 476 ± 25 μM). Under the assay conditions employed, the K_m for ATP was 207 ± 22 μM in platelet membranes. Thus, upon variation of the substrate concentration from 50 to 500 μM, a shift in the IC_{50} by a factor of 2.75-fold is expected for a competitive inhibitor; the shift actually observed (2.47-fold) is in reasonable agreement with this prediction. We have also carried out this assay with the combination of IC1 and IIC2 by employing 0.5 and 5 mM ATP (because the combination of IC1 and IIC2 has a higher K_m for ATP; see refs *4*−*6*) and measured shifts in the IC_{50} for oATP that are consistent with competitive inhibition (IC_{50} = 25 ± 3.5 and 46.1 ± 9.3 μM with 0.5 and 5 mM ATP, respectively). Previously, the competitive nature of oATP-dependent inhibition has been characterized by employing adenylyl cyclase partially purified from bovine brain by affinity chromatography on calmodulin−Sepharose (presumably enriched in the type II enzyme; *18*) and adenylyl cyclase solubilized from bovine caudate nucleus (presumably containing at least type I and type II adenylyl cyclase; *19*) and from bovine cerebral cortex. The K_i value for oATP was reported to be in the range of 40−200 μM; the affinity estimated in our experiments is in reasonable agreement with these reports. The aldehyde groups of oATP are capable of forming Schiff bases with the ϵ-amino group of lysine residues; thus, if a lysine residue in the ATP-binding pocket of adenylyl cyclase is accessible, inhibition of adenylyl cyclase by oATP should be quasi-irreversible. This was tested by preincubating platelet membranes with either ATP or oATP; after removal of the nucleotides, substrate was added and forskolin-stimulated enzyme activity was determined (Figure 1B). Irrespective of whether the preincubation was carried out in the presence of oATP alone (Figure 1B, first set of bars) or oATP and forskolin (Figure 1B, second set of bars), we observed an inhibition by >60% in membranes treated with oATP. This

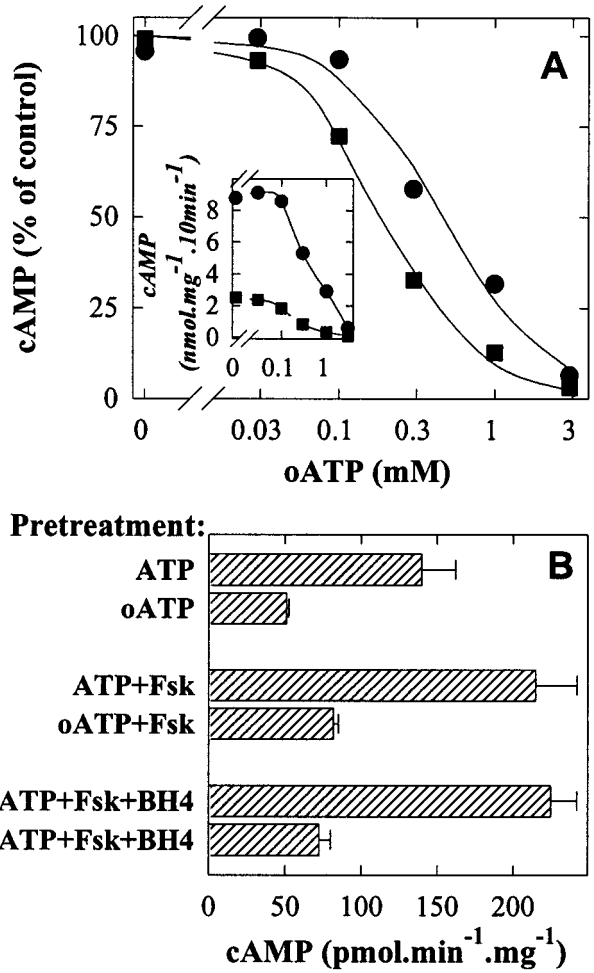

FIGURE 1: Inhibition of platelet adenylyl cyclase activity by oATP. (A) Platelet membranes (15 μg) were incubated in the absence and presence of the indicated concentrations of oATP for 10 min at 20 °C in 50 μL of substrate solution containing 50 μM forskolin, 10 mM $MgCl_2$, and 0.05 (■) or 0.5 mM [α-^{32}P]ATP (●) (specific activity of 400 and 40 cpm/pmol, respectively). Data are expressed as a percentage of the activity determined in the absence of oATP to account for the large difference in activity; the absolute level of cAMP formation is shown in the inset. Shown are the means of duplicate determinations in a representative experiment which was reproduced twice. (B) Platelet membranes were preincubated in the presence of 1 mM ATP (bar 1), 1 mM oATP (bar 2), the combination of 1 mM ATP and 50 μM forskolin (bars 3 and 5), or 1 mM oATP and 50 μM forskolin (bars 4 and 6) in buffer [50 mM Hepes·NaOH (pH 7.5), 1 mM EDTA, and 10 mM $MgCl_2$] for 20 min at 20 °C. Thereafter, the membranes were either sedimented immediately (bars 1−4) by centrifugation (10 min at 50000*g*) or first placed on ice and reduced with borohydride (bars 5 and 6) as described in Materials and Methods. After two washes, the membranes were resuspended and the amount of adenylyl cyclase was determined as described for panel A. Data are means of three independent experiments carried out in duplicate; error bars indicate the standard deviation (SD).

suggests that forskolin did not enhance binding of oATP during the preincubation. Similarly, if the Schiff base was reduced by the sequential addition of $NaCNBH_3$ and $NaBH_4$ at the end of the preincubation (prior to removal of the nucleotides), the oATP-induced inhibition was only marginally enhanced (to about 70%; Figure 1B, third set of bars), indicating that there was little dissociation of oATP during the washing steps employed to remove the free nucleotides.

Labeling of IIC2 with [α-^{32}P]oATP. On the basis of the observations summarized above, we concluded that [α-^{32}P]-

oATP may be a suitable ligand for labeling the ATP binding site of adenylyl cyclase. If the isolated domains were incubated with [α-^{32}P]oATP, labeling of IIC2 was readily detectable while the extent of incorporation into IC1 was low (Figure 2A). If the two domains were combined, labeling of IC1 and IIC2 was modestly enhanced (1.5 ± 0.2-fold); in contrast, addition of forskolin (Figure 2A) and of active GTPγS-liganded $rG_{s\alpha-s}$ (not shown) did not enhance the incorporation of [α-^{32}P]oATP. A similar pattern (i.e., labeling of IIC2 but not of IC1) was obtained if the incubation was carried out with $^{8}N_3$-[α-^{32}P]ATP; this analogue was previously used to map the ATP-binding site on purified adenylyl cyclase (*20*). In contrast, Bz_2[α-^{32}P]ATP was not incorporated into IIC2. This failure cannot be ascribed to UV-induced denaturation of the protein, because irradiation of IC1 and of IIC2 in the absence of adenine nucleotides inhibited catalysis by only ∼25% (not shown).

The incorporation of [α-^{32}P]oATP into IIC2 may have resulted from nonspecific attachement to lysine residues on the surface of the protein. The following findings rule out this possibility. (i) The specificity of [α-^{32}P]oATP incorporation was examined by testing the ability of ATP to suppress the labeling of IIC2; ATP inhibited the incorporation of [α-^{32}P]oATP (Figure 2B) with an IC_{50} of 1.1 ± 0.4 mM ($n = 3$). In contrast, the P-site inhibitor 2′,3′-ddA failed to affect the labeling of IIC2 up to 1 mM irrespective of whether the incubation was carried out in the absence or presence of pyrophosphate (not shown). (ii) The labeling stoichiometry was determined in a saturation experiment; increasing concentrations of [α-^{32}P]oATP were incubated with 20 μg of IIC2 (i.e., ∼690 pmol), and the Schiff base was converted to a covalent bond by reduction with borohydride and the protein denatured in the presence of trichloroacetic acid to release any noncovalently attached nucleotide (Figure 2C). The binding isotherm was reasonably well described by a rectangular hyperbola such that a linear plot was obtained upon Scatchard transformation (Figure 2B, inset). The K_d estimate was 0.6 ± 0.3 mM ($n = 3$), and the calculated B_{max} was 249 ± 33 pmol, corresponding to a stoichiometry of incorporation of about 0.36. (iii) Following incorporation of [α-^{32}P]oATP into IIC2, the protein was cleaved with CNBr; upon electrophoretic resolution, a single radioactively labeled fragment of 6.5 kDa was detected (not shown). Taken together, these observations indicate that [α-^{32}P]oATP interacts with a low-affinity ATP-binding site on IIC2.

Effect of Mg^{2+} and Mn^{2+} on the Labeling of IIC2 by oATP and by FITC. For enzymatic activity, adenylyl cyclase requires a divalent cation, Mg^{2+} being presumably the physiological ligand; however, Mn^{2+} efficiently substitutes for Mg^{2+} and increases the rate of catalysis (*1*, *11*). We have therefore examined whether oATP binding to IIC2 depends on the presence of a divalent cation. In the absence of any divalent cation, oATP was incorporated into IIC2 at low but readily detectable levels. Mg^{2+} modestly stimulated this labeling (∼1.4-fold at 30 mM), but Mn^{2+} was much more effective in supporting the incorporation of oATP into IIC2 (Figure 2D). The maximum stimulation level was observed in the range of 10−30 mM Mn^{2+}; at concentrations exceeding 30 mM, the extent of Mn^{2+} labeling decreased again (not shown). While the effect of Mg^{2+} was too small to reliably calculate an EC_{50} from densitometric scans, we estimated half-maximum enhancement to be 3.82 ± 0.57 mM total

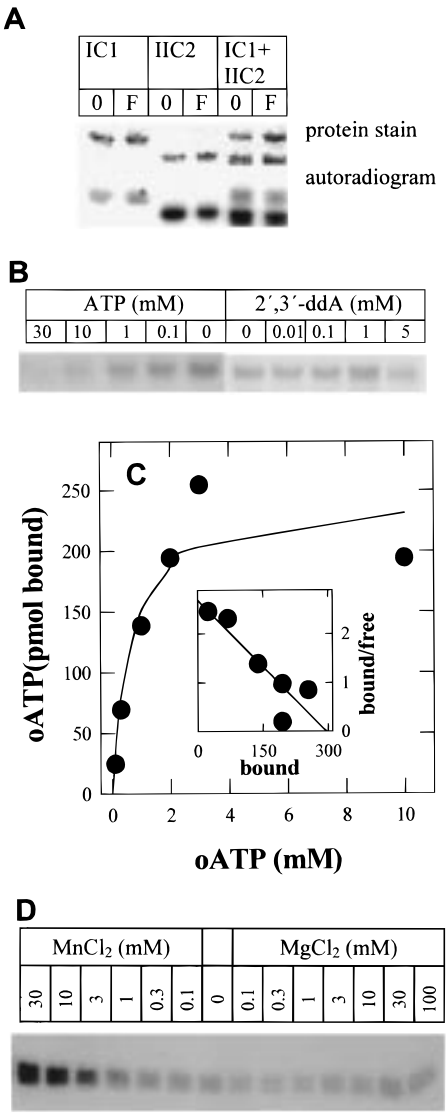

FIGURE 2: Covalent labeling of IIC2 by [α-^{32}P]oATP. (A) IC1 and IIC2 (each at ∼0.5 μg/assay) were incubated separately or in combination as indicated with 100 μM [α-^{32}P]oATP (B, specific activity of ∼400 cpm/pmol) in 20 μL of buffer [50 mM Hepes·NaOH (pH 7.5), 1 mM EDTA, and 10 mM $MgCl_2$] for 10 min at 20 °C. Where indicated by the letter F, forskolin was present at 50 μM. For [α-^{32}P]oATP, the incorporation was catalyzed by the sequential addition of $NaCNBH_3$ and $NaBH_4$ as described in Materials and Methods. The proteins were electrophoretically resolved and visualized by staining with Coomassie Blue (top); the incorporated radioactivity was detected by autoradiography (bottom; Kodak X-Omat, 12 h exposure at −80 °C). (B) IIC2 (0.5 μg/assay) was incubated with 100 μM [α-^{32}P]oATP in the absence and presence of the indicated concentrations of ATP and 2′,3′-ddA. Assay conditions were as outlined for panel A. (C) Stoichiometry of [α-^{32}P]oATP binding to IIC2. Purified IIC2 (20 μg/assay) was incubated in 25 μL of buffer [50 mM Hepes·NaOH (pH 7.5), 1 mM EDTA, and 5 mM $MnCl_2$] containing the indicated [α-^{32}P]-oATP concentrations (specific activity of 20−170 cpm/pmol). After 20 min at 20 °C, $NaCNBH_3$ and $NaBH_4$ were added as described for panel A; the protein was denaturated by the addition of 0.5 mL of 2% SDS and 0.5 mL of 30% trichloroacetic acid and subsequently trapped on nitrocellulose filters. Data are means of duplicate determinations in a representative experiment; two additional experiments gave similar results. The inset of panel C shows the Scatchard tranformation of the data. (D) Effect of Mg^{2+} and of Mn^{2+} on the incorporation of [α-^{32}P]oATP into IIC2. IIC2 (0.5 μg/assay) was incubated with 100 μM [α-^{32}P]oATP in the absence and presence of the indicated total concentrations (millimolar) of Mg^{2+} and of Mn^{2+}. Assay conditions were as outlined for panel A.

Mn^{2+} (i.e., ~2.8 mM free Mn^{2+} if chelation by 1 mM EDTA is accounted for) from three independent experiments.

In many proteins, FITC is capable of interacting with the ATP-binding site (*21*, *22*). The reactive isothiocyanate group can form thiourea derivatives with free amino groups and is therefore covalently incorporated into lysine residues. Because our observations showed that oATP was incorporated into IIC2 and because FITC treatment of IIC2 inhibited cAMP formation by IC1 and IIC2 ($IC_{50} = 82 \pm 18$ μM), we surmised that FITC may also label IIC2. In the absence of metal ions, only low levels of FITC were incorporated into IIC2; however, Mg^{2+} and, to a much larger extent, Mn^{2+} promoted labeling of IIC2 by FITC (Figure 3A,B). For Mn^{2+}, an EC_{50} value of 2.44 ± 0.75 mM was estimated from the data shown in the lower panel of Figure 3B. Again, we consider the effect of Mg^{2+} to be too small to derive a reliable affinity estimate. The control experiment carried out with IC1 showed that labeling of IC1 by FITC was barely detectable (Figure 3A); Mg^{2+} and Mn^{2+} caused a very modest increase which was comparable in magnitude (bottom panel in Figure 3A). The extent of incorporation of FITC into IIC2 was reduced upon addition of IC1 (Figure 3A, last three lanes), suggesting that upon association of the two domains the ATP-binding site is less accessible to FITC. If FITC interacted with the ATP-binding site of IIC2, ATP would be expected to inhibit labeling; this was the case. As can be seen from Figure 3C, both ATP ($IC_{50} = 3.92 \pm 0.98$ mM) and Bz_2ATP ($IC_{50} = 0.85 \pm 0.15$ mM) suppressed FITC labeling in a concentration-dependent manner. It is worth noting that, because of the irreversible nature of FITC labeling, the apparent IC_{50} of ATP and of Bz_2ATP was dependent on the incubation time and progressively decreased with increasing labeling periods. We have also tested oATP, which potently suppressed FITC labeling of IIC2; in contrast, 2′,3′-ddA and adenosine were ineffective up to 1 mM (data not shown).

Fluorescence Enhancement of TNP-ATP by IIC2. Although $Bz_2[\alpha\text{-}^{32}P]ATP$ was not photoincorporated into IIC2, the FITC labeling experiments indicated that Bz_2ATP was capable of interacting with IIC2. This observation implies that IIC2 can bind ATP analogues that are subsituted on the ribose ring. We have therefore used TNP-ATP to study metal ion-promoted binding of ATP to IIC2. Upon excitation at 408 nm, TNP-ATP displays low-intensity fluorescence with a broad peak at 550−560 nm in aqueous solution (see refs *23*−*25* and the corresponding trace 2 in Figure 4A). The fluorescent properties are greatly enhanced, and the emission peak displays a blue shift (to 540 nm) in a hydrophobic environment such as in less polar solvents (e.g., in dimethylformamide) or upon binding to a protein (*23*−*25*). The appropriate control traces are shown in Figure 4A; the combination of buffer and CII was devoid of fluorescence (trace 1), and the background fluorescence of 100 μM TNP-ATP (trace 2) is modestly enhanced by the addition of 24 μM IIC2 (trace 3), of 10 mM $MgCl_2$ (trace 4), or of 10 mM $MnCl_2$ (trace 5). If IIC2 was combined with 10 mM $MgCl_2$, there was a minor increase in the fluorescence of TNP-ATP (trace 6); in contrast, addition of 10 mM $MnCl_2$ to IIC2 and TNP-ATP greatly stimulated light emission (trace 7).

To estimate the affinity of Mn·TNP-ATP for IIC2, we determined the fluorescence of increasing concentrations of TNP-ATP in the absence and presence of IIC2; Figure 4B shows a representative saturation isotherm for TNP-ATP at 30 μM IIC2 and 0.5 mM $MnCl_2$ obtained by subtracting the baseline fluorescence of TNP-ATP (▼ in the inset of Figure

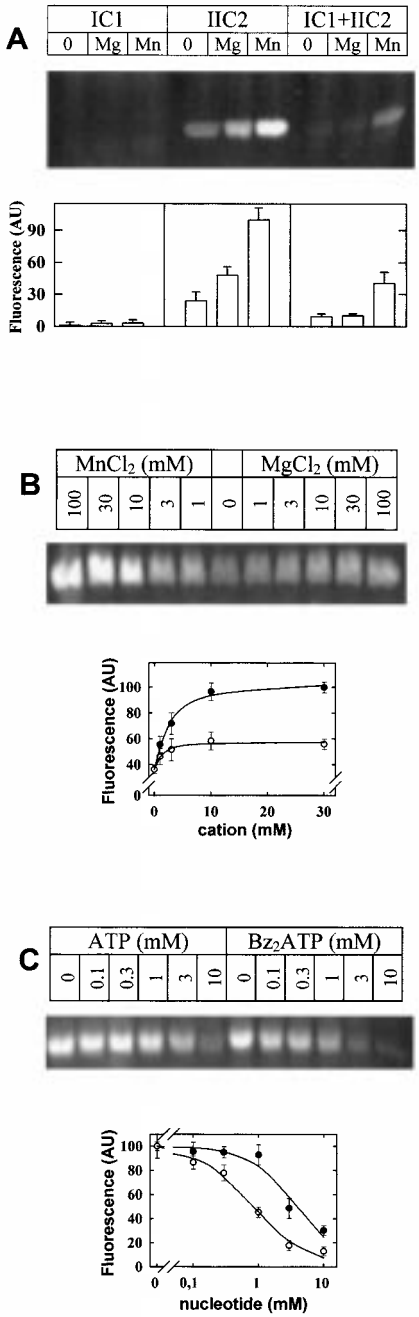

FIGURE 3: Labeling of IC1 and of IIC2 by FITC. (A) IC1 and IIC2 (each at ~0.5 μg/assay) were incubated separetely or in combination as indicated with 100 μM FITC in 20 μL of buffer containing 50 mM Hepes·NaOH (pH 7.5), 1 mM EDTA, and where applicable either 10 mM $MgCl_2$ or $MnCl_2$ for 10 min at 20 °C in the dark followed by electophoresis on an SDS−polyacrylamide gel; incorporation of FITC into the proteins was visualized with UV light as outlined in Materials and Methods. (B) IIC2 (~0.5 μg/assay) was reacted with FITC in the presence of the indicated total concentration (millimolar) of $MgCl_2$ (○) or $MnCl_2$ (●) as described for panel A. (C) IIC2 (~0.5 μg/assay) was reacted with FITC in the presence of 10 mM $MnCl_2$ and the indicated concentrations (millimolar) of ATP (●) or Bz_2ATP (○); assay conditions were as described for panel A. Diagrams shown under the fluorograms were obtained by averaging the fluorescence recorded in three independent experiments; error bars represent the SD.

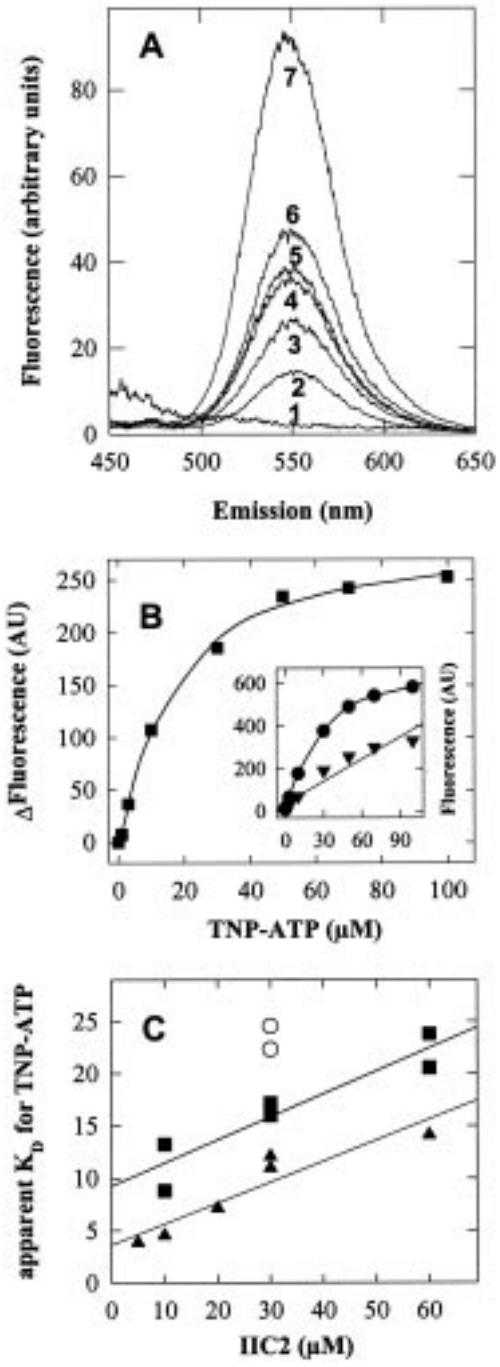

FIGURE 4: Fluorescence spectra of IIC2 and TNP-ATP in the absence and presence of Mg^{2+} and Mn^{2+} (A) and saturation of the IIC2-dependent increase in TNP-ATP fluorescence in the presence of Mn^{2+} (B). (A) The excitation monochromator was set at 408 nm, and the emission monochromator was changed at a rate of 200 nm/s. The following spectra were recorded sequentially in 200 μL of buffer [20 mM Hepes·NaOH (pH 7.5) and 1 mM EDTA]: trace 1, CII (24 μM); trace 2, 100 μM TNP-ATP; trace 3, 24 μM IIC2 and 100 μM TNP-ATP; traces 4 and 5, 100 μM TNP-ATP in buffer containing 10 mM $MgCl_2$ and 10 mM $MnCl_2$, respectively; and traces 6 and 7, 24 μM IIC2 and 100 μM TNP-ATP in buffer containing 10 mM $MgCl_2$ and 10 mM $MnCl_2$, respectively. (B) IIC2 (30 μM) was incubated in buffer containing the indicated concentrations of TNP-ATP and 0.5 mM free $MnCl_2$. The excitation wavelength was 408 nm; emission was recorded at 540 nm. Data points (■) correspond to the difference in fluorescence recorded in the absence (inset ▼) and presence of IIC2 (inset, ●). (C) The concentration of IIC2 was varied as indicated, and the apparent K_D for TNP-ATP was determined as described for panel B in the absence (○) and presence of 0.5 (■) and 2 mM (▲) Mn^{2+}. Data are from independent experiments carried out with two different preparations of IIC2.

4B) from the fluorescence recorded in the presence of IIC2 (● in the inset of Figure 4B). An apparent K_D of 16 μM was calculated. However, this approach underestimates the true affinity because of the depletion of free TNP-ATP that occurs at low concentrations. Therefore, the apparent K_D was determined over a range of IIC2 concentrations covering 5−60 μM in the presence of 0.5 and 2 mM free Mn^{2+}. Figure 4C summarizes these experiments. It is evident that the apparent K_D decreases as the concentration of IIC2 is lowered. The *y*-intercepts yield the K_D estimates at an infinitely low concentration of IIC2 (i.e., in the absence of depletion of TNP-ATP). These data also show that the affinity of IIC2 for TNP-ATP is increased by Mn^{2+}; the intercept is 9 and 3 μM at 0.5 and 2 mM Mn^{2+}, respectively, while the slopes of the regression lines (which reflect the stoichiometry of interaction between TNP-ATP and IIC2) do not differ appreciably. Finally, in the complete absence of Mn^{2+}, addition of IIC2 still increases the fluorescence of TNP-ATP (cf. traces 2 and 3 in Figure 4A). However, the affinity of TNP-ATP is lower (○ in Figure 4C) than in the presence of Mn^{2+}.

The fluorescence observed in the presence of Mn^{2+} was due to the interaction of TNP-ATP with the ATP-binding site of IIC2 because it was reversed, if increasing concentrations of ATP were added to the reaction mixture (Figures 5A and 6); the kinetics of fluorescence reversal by ATP were rapid and comparable to those induced by chelation of the metal ion (Figure 6A). The calculated IC_{50} value for ATP in the presence of Mn^{2+} was 2.9 ± 0.4 mM (● in Figure 5B). We rule out the possibility that the inhibition by ATP merely reflects its ability to chelate Mn^{2+}, because the IC_{50} estimated for Mn·ATP (i.e., ATP that had been combined with equimolar Mn^{2+} concentrations prior to adding the solution to the cuvette) was similar (not shown). Similarly, ATP also suppressed the IIC2-dependent enhancement of TNP-ATP fluorescence in the absence of Mn^{2+}, albeit with lower potency (○ in Figure 5B). This inhibition reflected competition for a common site, because the effect of 10 mM ATP was lost, if the concentration of TNP-ATP was raised to 300 μM (△ in Figure 5B).

In contrast to ATP, adenosine failed to inhibit TNP-ATP fluorescence in concentrations up to 11 mM (■ in Figure 5B); a similar finding was also obtained with 2′,3′-ddA (not shown). The Mn^{2+} requirement of IIC2 for enhancing the fluorescence of TNP-ATP was further tested by raising the concentration of free Mn^{2+} in a stepwise manner (Figure 6A). The increase in light emission was observed essentially instantaneously and was reversibly inhibited by addition of equimolar EDTA. The data summarized in Figure 6B indicate that the half-maximum effect was observed at ~1 mM free Mn^{2+}.

DISCUSSION

The recently solved crystal structure of the complex of a C1 and a C2 domain indicates that the ATP binding site is formed by surfaces that are in the cleft between the two domains; in addition, a single Mg^{2+} was visualized in the crystal of the C1−C2 heterodimer, and this was liganded to two aspartate residues of C1 (*9*). However, adenylyl cyclase requires Mg^{2+} or Mn^{2+} in excess of ATP for catalysis (*11*). Moreover, the active site of DNA polymerases contains two

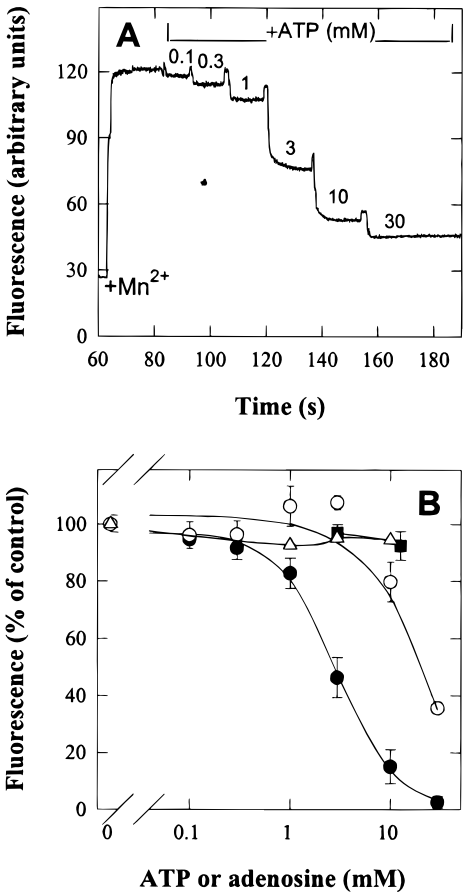

FIGURE 5: ATP-induced reversal of the Mn^{2+}-dependent fluorescence of IIC2 and TNP-ATP. (A) IIC2 (24 μM) was incubated with 100 μM TNP-ATP in 200 μL of buffer [20 mM Hepes·NaOH (pH 7.5) and 1 mM EDTA]; at the time points indicated by the injection artifact, Mn^{2+} was added to give a free concentration of 7 mM, and subsequently, ATP was added in a cumulative manner to give the indicated final ATP concentrations (in millimolar). Changes in fluorescence were recorded as outlined in the legend of Figure 4. (B) Concentration-dependent effect of ATP (●, ○, and △) and of adenosine (■) on the fluorescence of 100 μM (●, ○, and ■) and 300 μM TNP-ATP (△) bound to IIC2 (30 μM) in the absence (○ and △) and presence of 7 mM free Mn^{2+} (● and ■); the fluorescence recorded in the absence of IIC2 has been subtracted. Data are expressed as a percentage to normalize for the difference in the absolute level of fluorescence. Data are means of three to five independent experiments that were carried out in a manner like that described for panel A; error bars indicate the SD.

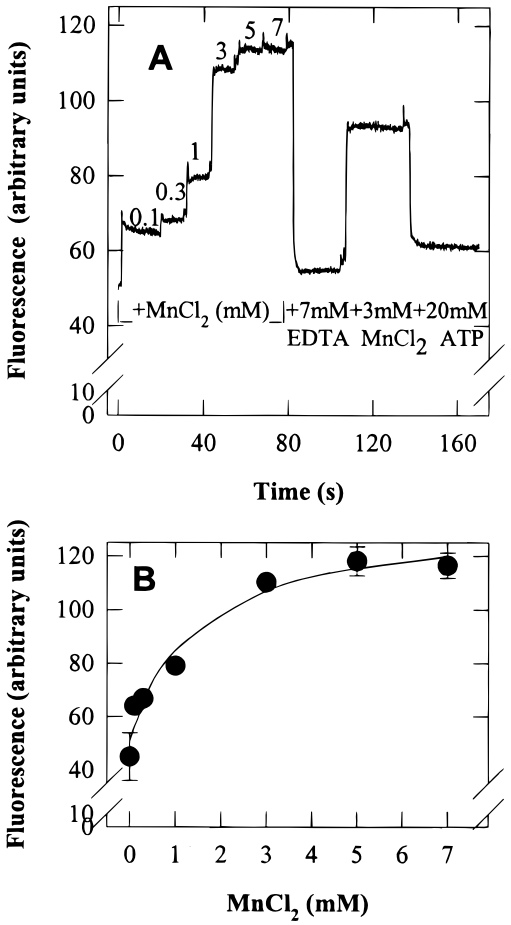

FIGURE 6: Mn^{2+}-induced change in the fluorescence of IIC2 and TNP-ATP. (A) IIC2 (24 μM) was incubated with 100 μM TNP-ATP in 200 μL of buffer [20 mM Hepes·NaOH (pH 7.5) and 1 mM EDTA]; at the time points indicated by the injection artifact, Mn^{2+} was added in a cumulative manner to give the concentrations in excess of EDTA as indicated followed by the sequential addition of EDTA (to give a final concentration of 8 mM), of Mn^{2+} (to give a concentration of 3 mM in execss of EDTA), and of ATP (to give a concentration of 20 mM). The excitation monochromator was set at 408 nm; emission was recorded at 540 nm, and data at the time points were sampled every 10 ms. (B) Concentration−response curve for the Mn^{2+}-induced fluorescence increase. Data are means of three independent experiments; error bars indicate the SD.

metal ions termed A and B (*26*−*28*); metal ion A presumably polarizes the 3′-OH group, and metal ion B interacts with the three phosphates of the incoming nucleotide and is likely to correspond to the Mg^{2+} present in the C1−C2 heterodimer (*4*). Thus, a second metal binding site is to be postulated in the active site of adenylyl cyclase on the basis of the analogy of the reaction mechanism that is catalyzed by DNA polymerases (3′,5′-diester bond between two nucleotides) and by adenylyl cyclases (formation of an intramolecular diester). This work shows that C2 carries a metal ion-binding site which prefers Mn^{2+} over Mg^{2+}; this conclusion is based on three lines of evidence. (i) oATP and (ii) FITC labeling of IIC2 was more effectively promoted by Mn^{2+} than by Mg^{2+}. (iii) Similarly, Mn^{2+}, and to a much lesser extent Mg^{2+}, enhanced the fluorescence of TNP-ATP in the presence of IIC2. We therefore propose that the metal ion binding site residing on IIC2 corresponds to the second binding site; by binding to this site, the metal ion may participate in catalysis by activating the 3′-hydroxyl and/or by stabilizing the pentavalent transition state of the α-phosphorus. An earlier observation also suggests that there is a metal binding site on the C2 domain; levels of catalytic activity that are sufficient to rescue an *E. coli* strain deficient in adenylyl cyclase can be observed after expression of C2 but not of after expression of C1 (*3*). If C2 lacked a metal binding site, it would be entirely devoid of enzymatic activity and could therefore not possibly support bacterial growth.

Half-maximal effects of Mn^{2+} were observed in the range of 1−3 mM; this concentration is more than 1 order of magnitude higher than those required to support catalysis by a VC1−IIC2 heterodimer ($EC_{50} \sim 0.1$ mM; see ref *29*) or by a IC1−IIC2 heterodimer ($EC_{50} \sim 0.1$ mM; data not shown). This suggests that the C1 domain enhances the affinity of the C2 domain for Mn^{2+}. Mutations have been generated that only modestly affect the K_m for Mg·ATP but that increase 100-fold the concentration of Mg^{2+} required

to activate catalysis (*29*); these mutations affect residues in the C1 domain that are thought to support the orientation of the aspartic acid residues required for Mg^{2+} and have a much less pronounced effect on the Mn^{2+} requirement (*29*, *30*). These data are consistent with our interpretation that binding of Mn^{2+} is predominantly supported by the C2 domain. Earlier experiments have shown that chelation of free metal ions by EGTA inhibits catalysis by adenylyl cyclase. Enzymatic activity can be restored by Mn^{2+} but not by Mg^{2+}; these observations have led to the proposal that, in its native conformation, adenylyl cyclase contains a tightly bound metal ion, possibly Mn^{2+} (*31*, *32*). Although this hypothesis was put forth some 25 years ago, the biological significance of Mn^{2+} in the regulation of cAMP formation remains unclear.

P-Site inhibitors are ribose-modified (deoxy- and 3′-phosphorylated) adenosine analogues which suppress catalysis by acting directly on adenylyl cyclase (see ref *33* for the structure−activity relationship). On the basis of kinetic arguments, two models have been put forth to explain the mechanism of P-site inhibition; in the allosteric model, P-site inhibitors interact with a site distinct from the catalytic site such that substrate and inhibitor may be bound simultaneously (*34*, *35*). Alternatively, P-site inhibitors were proposed to bind to the catalytic site where they act as dead-end inhibitors (*36*). The current evidence favors the latter model; P-site analogues act as noncompetitive inhibitors with respect to the forward reaction but are competitive with cAMP in the reverse reaction, i.e., the synthesis of ATP from cAMP and pyrophosphate (*37*). Furthermore, a P-site inhibitor is bound to the presumed catalytic site in the crystal of the C1−C2 heterodimer (*9*). Finally, Ap(CH_2)pp, an ATP analogue which cannot serve as a substrate, binds with a 1:1 stoichiometry to the C1−C2 heterodimer, and this is not inhibited by 2′,3′-ddA, presumably because binding of 2′,3′-ddA to the active site requires pyrophosphate (*37*). It is thus not unexpected that 2′,3′-ddA and adenosine failed to inhibit the interaction of IIC2 with ATP analogues. Similarly, the fact that pyrophosphate did not affect the binding of oATP to IIC2 in the presence of P-site inhibitors can be rationalized because in the C1−C2 heterodimer pyrophosphate is held in place by a P-loop connecting the β1-sheet and the α1-helix of C1 (*9*).

Previous experiments have failed to detect binding of radiolabeled Ap(CH_2)pp to either isolated VC1 or IIC2 (*4*); in contrast, our findings indicate that binding of oATP to IIC2 alone can be observed. We stress that this is only a seeming contradiction; with the notable exception of TNP-ATP, the affinity of ATP analogues for the isolated domains is low, and hence, binding levels determined by equilibrium dialysis would require larger amounts of protein than those employed in ref *4*. We also rule out the possibility that binding of oATP to IIC2 is nonspecific because it is suppressed by ATP and regulated by Mn^{2+} and because it is incorporated into the protein with a reasonable stoichiometry. The observation that the reduction with BH_4 results in a stoichiometry of incorporation of less than 1:1 (i.e., 0.36) can presumably be attributed to the yield of the chemical reaction, to the fact that isolated IIC2 is a homodimer (*6*), and to the fact that some of the protein is inactive (*38*).

Bz_2ATP was only covalently incorporated into IC1 but not into IIC2 regardless of whether the labeling reaction was carried out with the isolated domains or after their combination; the failure of Bz_2ATP to label IIC2 when complexed to IC1 is to be expected on the basis of the structure of the heterodimer, because the benzoylbenzoic moiety is presumably oriented toward C1 in the complex (*9*). In contrast, while Bz_2ATP (and the related analogue TNP-ATP) did bind to IIC2, Bz_2ATP was not covalently incorporated; the likely explanation for this discrepancy lies in the assumption that no reactive group of IIC2 is available in the close vicinity of the radical generated upon UV photolysis. These findings highlight an obvious caveat in the interpretation of labeling data.

The mechanism that leads to activation or inhibition of catalysis is not known (*39*); several experimental findings indicate that binding of ATP is not rate-limiting: activators have only modest effects on the affinity of ATP, the release of product (cAMP and pyrophosphate) is in part rate-limiting (*38*), and it is likely that activators stabilize the transition state (*8*). Nevertheless, the stimulation of domain association is an important effect of activators (*6*), and constitutive activation of adenylyl cyclase is induced by a point mutation that is thought to promote the interaction of C1 and C2 (*40*). The fluorescence method presented here may be useful in studying the interaction of C1 and C2 domains, in particular the regulation of domain assocation by stimulatory (such as $G_{s\alpha}$, forkolin, calmodulin, and $\beta\gamma$-dimers) and inhibitory ligands ($G_{i\alpha}$ and $\beta\gamma$-dimers) as well as the effect of mutations and modifications (e.g., phosphorylation). This requires that the fluorescence of the complex of C2 and TNP-ATP is further enhanced by the addition of C1. This is currently being explored.

ACKNOWLEDGMENT

We thank A. Karel and E. Tuisl for assistance in preparing the artwork.

REFERENCES

1. Sunahara, R. K., Dessauer, C. W., and Gilman, A. G. (1996) *Annu. Rev. Pharmacol. Toxicol. 36*, 461−480.
2. Londos, C., and Wolff, J. (1977) *Proc. Natl. Acad. Sci. U.S.A. 74*, 5482−5486.
3. Tang, W.-J., and Gilman, A. G. (1995) *Science 268*, 1769−1772.
4. Dessauer, C. W., and Gilman, A. G. (1996) *J. Biol. Chem. 271*, 16967−16974.
5. Whisnant, R. E., Gilman, A. G., and Dessauer, C. W. (1996) *Proc. Natl. Acad. Sci. U.S.A. 93*, 6621−6625.
6. Yan, S.-Z., Hahn, D., Huang, Z. H., and Tang, W.-J. (1996) *J. Biol. Chem. 271*, 12342−12349.
7. Sunahara, R. K., Dessauer, C. W., Whisnant, R. E., Kleuss, C., and Gilman, A. G. (1997) *J. Biol. Chem. 272*, 22265−22271.
8. Zhang, G. Y., Liu, Y., Ruoho, A., and Hurley, J. H. (1997) *Nature 386*, 247−253.
9. Tesmer, J. J. G., Sunahara, R. K., Gilman, A. G., and Sprang, S. R. (1997) *Science 278*, 1907−1916.
10. Liu, Y., Ruoho, A., Rao, V. D., and Hurley, J. H. (1997) *Proc. Natl. Acad. Sci. U.S.A. 94*, 13414−13419.
11. Garbers, D. L., and Johnson, R. A. (1975) *J. Biol. Chem. 250*, 8449−8456.
12. Easterbrook-Smith, S. B., Wallace, J. C., and Keech, D. B. (1976) *Eur. J. Biochem. 62*, 125−130.
13. Hohenegger, M., and Makinose, M. (1992) *Eur. J. Biochem. 205*, 173−179.
14. Williams, N., and Coleman, P. S. (1982) *J. Biol. Chem. 257*, 2834−2841.
15. Nanoff, C., Boehm, S., Hohenegger, M., Schütz, W., and Freissmuth, M. (1994) *J. Biol. Chem. 269*, 31999−32007.

16. Hohenegger, M., Mitterauer, T., Nanoff, C., Voss, T., and Freissmuth, M. (1996) *Mol. Pharmacol. 49*, 73−80.
17. Hohenegger, M., Nanoff, C., Ahorn, H., and Freissmuth, M. (1994) *J. Biol. Chem. 269*, 32008−32015.
18. Westcott, K. R., Olwin, B. B., and Storm, D. R. (1980) *J. Biol. Chem. 255*, 8767−8771.
19. Winslow, J. W., and Neer, E. J. (1986) *J. Biol. Chem. 261*, 7626−7634.
20. Droste, M., Mollner, S., and Pfeuffer, T. (1996) *FEBS Lett. 391*, 209−214.
21. Fletterick, R. S., Bates, D. J., and Steitz, T. A. (1975) *Proc. Natl. Acad. Sci. U.S.A. 72*, 38−42.
22. Farley, R. A., Tran, C. M., Carilli, C. T., Haroka, D., and Shively, J. E. (1984) *J. Biol. Chem. 259*, 9532−9535.
23. Hiratsu, T. S., and Uchida, K. (1973) *Biochim. Biophys. Acta 320*, 635−647.
24. Grubmeyer, C., and Penefsky, H. S. (1981) *J. Biol. Chem. 256*, 7241−7249.
25. Watanabe, T., and Inesi, G. (1982) *J. Biol. Chem. 257*, 11510−11516.
26. Doublié, S., Tabor, S., Long, A. M., Richardson, C. C., and Ellenberger, T. (1998) *Nature 391*, 251−258.
27. Kiefer, J. R., Mao, C., Braman, J. C., and Beese, L. S. (1998) *Nature 391*, 304−307.
28. Steitz, T. A. (1998) *Nature 391*, 231−232.
29. Zimmermann, G., Zhou, D., and Taussig, R. (1998) *J. Biol. Chem. 273*, 19650−19655.
30. Tang, W.-J., Stanzel, M., and Gilman, A. G. (1995) *Biochemistry 34*, 14563−14572.
31. Johnson, R. A., and Sutherland, E. W. (1973) *J. Biol. Chem. 248*, 5114−5121.
32. Neer, E. J. (1979) *J. Biol. Chem. 254*, 2089−2096.
33. Desaubry, L., Soshani, I., and Johnson, R. A. (1996) *J. Biol. Chem. 271*, 14028−14034.
34. Yeung, S.-M. H., and Johnson, R. A. (1990) *J. Biol. Chem. 265*, 16745−16750.
35. Johnson, R. A., and Soshani, I. (1990) *J. Biol. Chem. 265*, 16967−16974.
36. Florio, V. A., and Ross, E. M. (1983) *Mol. Pharmacol. 23*, 195−202.
37. Dessauer, C. W., and Gilman, A. G. (1997) *J. Biol. Chem. 271*, 27787−27795.
38. Dessauer, C. W., Scully, T. T., and Gilman, A. G. (1997) *J. Biol. Chem. 272*, 22272−22277.
39. Skiba, N., and Hamm, H. (1998) *Nat. Struct. Biol. 5*, 88−92.
40. Parent, C. A., and Devreotes, P. N. (1996) *J. Biol. Chem. 271*, 18333−18336.

BI981441M